



Numerical investigation of natural convection in a cavity using an open geometry

Boris Brangeon, Alain Bastide, Patrice Joubert, Michel Pons

► To cite this version:

Boris Brangeon, Alain Bastide, Patrice Joubert, Michel Pons. Numerical investigation of natural convection in a cavity using an open geometry. IndoorAir 2011, Jun 2011, Austin, United States. p8. <hal-00643466>

HAL Id: hal-00643466

<https://hal.science/hal-00643466v1>

Submitted on 22 Nov 2011

HAL is a multi-disciplinary open access archive for the deposit and dissemination of scientific research documents, whether they are published or not. The documents may come from teaching and research institutions in France or abroad, or from public or private research centers.

L'archive ouverte pluridisciplinaire **HAL**, est destinée au dépôt et à la diffusion de documents scientifiques de niveau recherche, publiés ou non, émanant des établissements d'enseignement et de recherche français ou étrangers, des laboratoires publics ou privés.



HAL Authorization

Numerical investigation of natural convection in a cavity using an open geometry

Boris Brangeon^{1,*}, Alain Bastide¹, Patrice Joubert² and Michel Pons³

¹PIMENT, Université de La Réunion, 117 Avenue du Général Ailleret 97430 Le Tampon, France.

²LEPTIAB, Université de La Rochelle, Avenue M. Crépeau, 17042 La Rochelle Cedex 1, France.

³LIMSI CNRS UPR3251, BP 133, 91403 Orsay Cedex, France.

*Corresponding email: boris.brangeon@univ-reunion.fr

SUMMARY

This paper presents a numerical investigation of airflow in an open geometry. The case under consideration is a room with two opposite and decentred openings which create a strong potential for ventilation. The building's characteristic dimensions are the following: $H=2.50$ m height and $W=6.50$ m width. A temperature difference between the walls and the outside air is fixed, resulting in a characteristic Rayleigh number (Ra) ranging from 10^5 to 10^7 . This room model proceeds from a benchmark exercise "ADNBATI" (<http://adnbati.limsi.fr>) coordinated by the "Centre National de la Recherche Française -CNRS-".

IMPLICATIONS

This paper presents and discusses the results of this numerical study. Velocity, temperature fields, as well as heat transfer at the walls are analyzed. Values of the Nusselt number and of the mass flow rate according to the Rayleigh number are established from these first results.

KEYWORDS

Direct Numerical Simulation, Natural convection, Open enclosures, Boundary conditions.

INTRODUCTION

For night cooling of buildings, two choices are possible: mechanical ventilation and/or natural ventilation. The latter mechanism is an efficient passive cooling process for moderate hot climates and is investigated in this paper to remove excessive heat accumulated during the day. In the present study, investigations are performed to simulate natural convection within a building model. The geometrical configuration is an open room with two opposite and decentred openings to create a strong potential for natural ventilation. The room model proceeds from a benchmark exercise "ADNBATI" (Stephan, 2010) coordinated by the "Centre National de la Recherche Française -CNRS-". This study is the first step in a global work (wall to fluid heat transfer, flow zones definition, turbulence model test and selection, radiative heat transfer, etc...), but here only natural convection is considered. The building characteristics dimensions are the followings: $H=2.50$ m height and $W=6.50$ m width (see Figure 1). The opening ratio H_1/H_2 equals 0.5. Ra is the Rayleigh number based on the cavity height H . A temperature difference between the inside walls and the outside air is fixed, resulting in a characteristic Rayleigh number ranging from 10^5 to 10^7 .

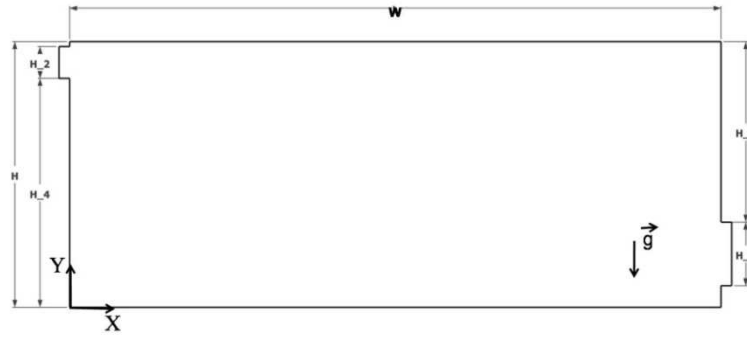


Figure 1. Cavity problem.

Table 1. Geometry characteristic parameters.

	Value [m]
Height low East opening H_1	0.6
Height low West opening H_2	0.3
Height wall East H_3	1.7
Height wall West H_4	2.15

METHODS

Governing equations

We consider a cavity of height H and width W traversed by an incompressible Newtonian viscous fluid of kinematic viscosity ν and thermal diffusivity κ (see figure 1). The fluid density ρ is assumed to depend only on temperature : $\rho = \rho_0[1 - \beta(T - T_0)]$, where β is the thermal expansion coefficient. The usual dimensionless Boussinesq 2D Navier-Stokes equations are then:

$$\frac{\partial u}{\partial x} + \frac{\partial v}{\partial y} = 0 \quad (1)$$

$$\frac{\partial u}{\partial t} + u \frac{\partial u}{\partial x} + v \frac{\partial u}{\partial y} = -\frac{\partial P_m}{\partial x} + PrRa^{-1/2}\nabla^2 u \quad (2)$$

$$\frac{\partial v}{\partial t} + u \frac{\partial v}{\partial x} + v \frac{\partial v}{\partial y} = -\frac{\partial P_m}{\partial y} + PrRa^{-1/2}\nabla^2 v + Pr\theta \quad (3)$$

$$\frac{\partial \theta}{\partial t} + u \frac{\partial \theta}{\partial x} + v \frac{\partial \theta}{\partial y} = Ra^{-1/2}\nabla^2 \theta \quad (4)$$

The corresponding equations are made dimensionless by introducing H , $U_{CN} = \kappa Ra^{1/2}/H$ (Bejan, 1984) and ΔT as reference quantities for length, velocity and temperature difference. The Prandtl number Pr is fixed to 0.71.

Boundary conditions

The wall's temperature is set to a constant temperature, T_w , higher than the outside temperature except for the frames of the openings for which an adiabatic condition is applied (see figure 1). A non-slip boundary condition is imposed on the velocity along all the walls.

Low East opening/ high West opening: the openings are framed, in order to take the thickness of the walls into account. The imposed conditions at the end of these frames ($X = -0.1$ m and $X = 6.6$ m) are the followings: if $\vec{V} \cdot \vec{n} < 0$ then $\theta = 0$, else $\frac{\partial \theta}{\partial x} = 0$.

The choice of the boundary conditions that must be applied to the velocity and the pressure is delicate for open geometries with natural convection flow. Indeed, the resulting thermosiphon

flow is the result of the balance between the forces due to buoyancy and the head losses between the low East and the high West openings of the cavity. However, no choice appears to be trivial to impose velocity or pressure conditions at the low East opening. We here propose the use of a boundary condition from a Stokes' phenomenon to the openings. We consider that at the low East opening, the following hypotheses are respected: the flow is steady and incompressible, the viscous terms are negligible and the rotational of the velocity equals zero. We can therefore relate the mass flow rate to the difference of pressure between the low East and the high West opening by the relation:

$$\int_{H_2} (p + \rho g z) \cdot dA - \int_{H_1} (p + \rho g z) \cdot dA = \int_{H_1} \frac{1}{2} \rho |V|^2 \cdot dA \quad (5)$$

This boundary condition is identical to the one which was proposed during a set benchmark in the framework of the network AMETH (Desrayaud, 2007) constituted of an asymmetrically-heated vertical channel, treated experimentally by Webb and Hill (Webb and Hill, 1989). The comparison of the two numerical simulations between different French research teams and our personal works, turns out to be conclusive for Ra equals to $5 \cdot 10^5$. The benchmark ADNBTI (Stephan, 2010) examines this issue and is currently subjected to a confrontation between numerical research codes and commercial codes. In our simulation, the boundary conditions are the following:

- at the low East opening: if $\vec{V} \cdot \vec{n} < 0$ then $P_m = -\frac{1}{2S_e^2} G^2$ where \vec{n} is exterior normal vector, G is mass flow rate and S_e is low East opening section. Locally, if $\vec{V} \cdot \vec{n} > 0$ then $P_m = -\frac{1}{2} |V|^2$, else $P_m = 0$.
- at the high West opening: a free-jet condition is imposed: $P_m = 0$.

Numerical approach: spatial and temporal discretization

The numerical code has been developed thanks to the environment OpenFOAM (OpenFOAM, 2010). The time derivatives in the momentum and in the energy equations are performed by a second-order backward differentiation. The convection terms are approximate using a second-order Adams-Bashford extrapolation method. The diffusion terms are implicitly treated. The resulting Helmholtz systems are solved by a direct solver. Finally, the general numerical scheme is the following:

$$\frac{3f^{n+1} - 4f^n + f^{n-1}}{2\Delta t} + 2 \left(\frac{\partial f u_j}{\partial x_j} \right)^n + \left(\frac{\partial f u_j}{\partial x_j} \right)^{n-1} = \left(\frac{\partial}{\partial x_j} \frac{\partial f}{\partial x_j} \right)^{n+1} \quad (6)$$

Pressure-velocity coupling is obtained by an incremental rotational projection method.

In the present study, a collocated finite volume method has been used. The case has been computed with a 1024×825 grid size. The local Reynolds number (Re) obtained is lower than 20 and the non-dimensional wall distance in terms of wall units (y^+) is less than 1. These quantities are displayed here for information on the quality of the mesh and will be submitted to an accurate study for more severe flows conditions for which turbulence models will be used. The dimensionless time step (Δt) varies from $1.25 \cdot 10^{-4}$ ($Ra = 10^5$) to $0.85 \cdot 10^{-4}$ ($Ra = 10^7$).

RESULTS AND DISCUSIONS

At least 60 dimensionless time units are used for this statistics calculation, in order to obtain the statistical values of u , v and θ . A steady laminar flow is obtained for $Ra=10^5$ and unsteady for $Ra=10^6$ and $Ra=10^7$.

Figure 2 displays the isotherms and streamlines fields for three values of the Rayleigh numbers: $Ra=10^5$, 10^6 and 10^7 . In the three cases, the flow which goes from the low East opening to the high West opening splits into two main flows. The main one is a cold jet, crawling on the floor surface until the West wall along which he finally goes up. The second moderate flow, goes right up along the East wall and joins the high West opening staying stuck to the ceiling. Between these two flows, two contrarotative cells exist, which progressively lengthen horizontally while Ra increases. The first one is localized above the jet, in the main part of the cavity ($c_{1,10^5}(x = 1.11; y = 0.47)$, $c_{1,10^6}(x = 0.70; y = 0.36)$, $c_{1,10^7}(x = 0.52; y = 0.40)$). The second one is located between the first cell and the heated surface of the ceiling ($c_{2,10^5}(x = 0.46; y = 0.70)$, $c_{2,10^6}(x = 0.71; y = 0.70)$). It becomes more and more intense. A third cell along the East wall which progressively disappears while Ra increases.

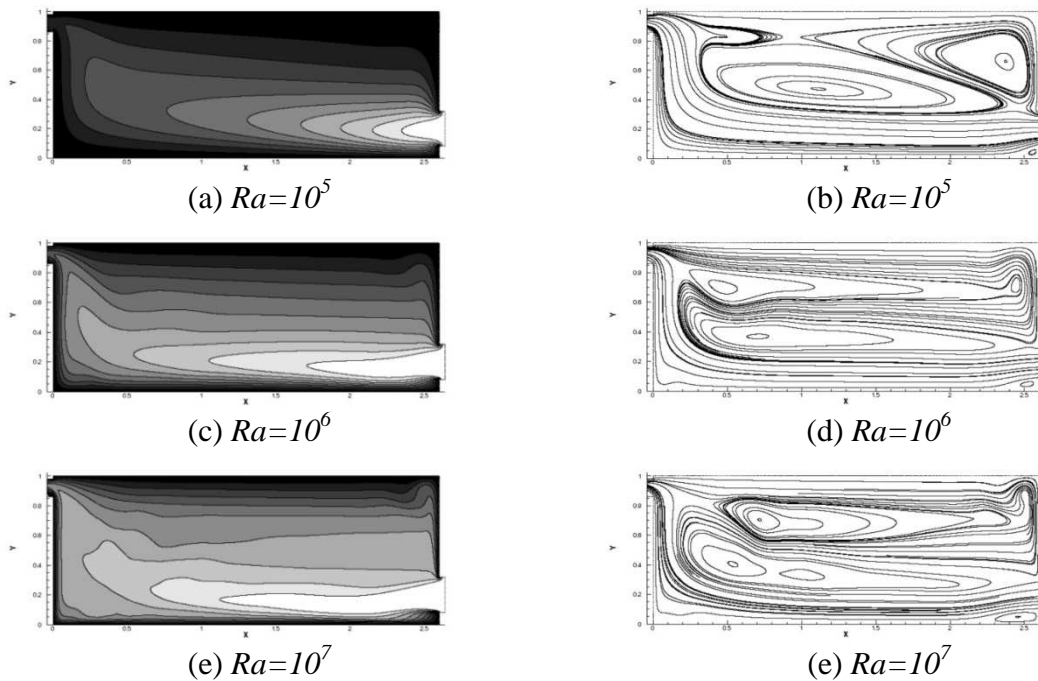


Figure 2. Average solutions. Left: average temperature field. Right: streamlines of average flow.

In addition, a penetration of fresh air becomes apparent and turns out to be stronger in the room as the Rayleigh number increases, that is to say when the convection acquires more importance compared to diffusion. The thickness of the boundary thermal layers decreases and the heart of the cavity cools down.

The third figure shows the evolution of the horizontal and vertical components of the velocity vector (respectively u and v) at the East opening (see figures 3(a) and 3(b)) and to the West opening (see figures 3(c) and 3(d)). The general velocity profiles at the East opening tends to distort itself and decreases rapidly when the temperature difference between the incoming air and the walls increases (see figure 3(a)). This may be explained by a vertical, Rayleigh-Benard type flow in the low part of the room, as these instabilities tend to contradict the inlet jet. At the West opening, the fluid re-enters the cavity within a height which can reach a

quarter of the outlet section for $Ra = 10^6$ - 10^7 . This phenomenon does not exist for the lower Rayleigh number.

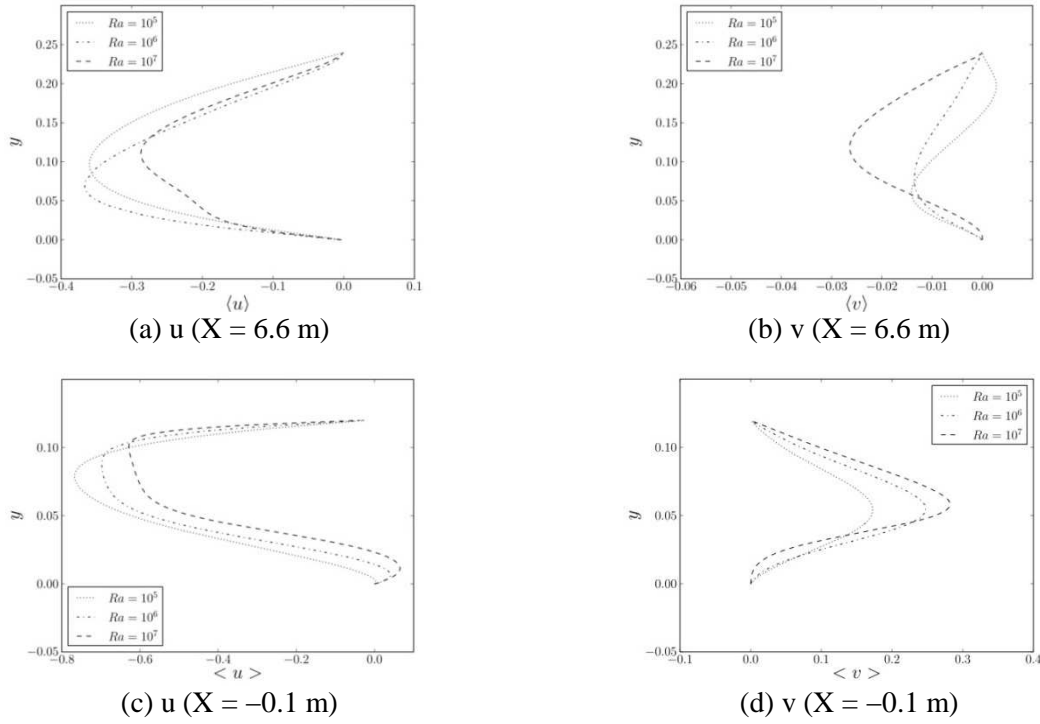


Figure 3. Average horizontal (left) and vertical (right) velocity profiles at inlet: 3(a) et 3(b) and outlet: 3(c) et 3(d).

The average values of the numbers of Nusselt Nu , obtained along the hot vertical and horizontal walls ($Nu_i = \frac{1}{H_i} \int \frac{\partial \theta}{\partial x} dn$), are reported in table 2(a) (Nu_F for the floor, Nu_R for the ceiling, Nu_O for the Western wall and Nu_E for the Eastern wall). The results indicate that the heat transfers are lower along the ceiling. For $Ra = 10^5$, the convective exchange on the vertical Western wall is lower than the one on the Eastern wall, even though the exchanges are balanced when Ra has superior values. It may be explained by the fact that for this value, the horizontal jet is weak and cannot drag the cold fluid up to the West wall. The average temperature of the fluid which is coming out from the high opening gives an indication on the quantity of total heat carried away outside by the fluid.

Quantitatively, we observe that the mass flow rate D_v remains low. It will be interesting to study if efficient rate of air exchange for the night cooling may be obtained when the number of Rayleigh has more important values.

Table 2. Average Nusselt number (a) and summary of average flow results (b).

Ra	10^5	10^6	10^7	Ra	10^5	10^6	10^7
Nu_F	3.60	8.01	17.95	G	0.023	0.021	0.018
Nu_R	0.80	1.49	2.97	D_v	0.223	0.654	1.775
Nu_O	1.58	7.21	17.41	τ	0.085	0.251	0.600
Nu_E	3.41	7.49	17.60	θ_m	0.850	0.700	0.550

(a)

(b)

CONCLUSION

A direct numerical simulation of the natural airflow in an open cavity has been presented and discussed. We choose a room model which will be used as a basis for other simulations in

order to expand our knowledge in regards to night cooling. The validation of the choice concerning the boundary condition on the inlet pressure has been realized on the basis of a comparison with the numerical data of the benchmark for $Ra = 5.10^5$ (Desrayaud, 2007). The first results that we are presenting in the benchmark configuration here ADNBTI (Stephan, 2010) will be confronted in a near future to other team's results especially concerning the values of the numbers of Nusselt and the obtained mass flow rate. The future perspectives would be, for example, to establish the evolution of the number of Rayleigh ($Nu = \alpha Ra^\gamma$). In order to realize a more realistic situation, $Ra = 10^8$ - 10^{10} , it would be indispensable to take turbulent models so as to obtain a time step compatible with parametrical simulations. A numerical approach of the flows through the large eddy simulation will be used for the superior numbers of Rayleigh to be found in the building.

ACKNOWLEDGEMENT

This work has been supported by French Research National Agency (ANR) through "Habitat intelligent et solaire photovoltaïque" program (project 4C n°ANR-08-HABISOL-019) and project "ADNBATT", financed by the Energy program of CNRS (PE09-3-2-1-1).

REFERENCES

- Bejan A. Convection heat transfer. John Wiley and Sons, 1984.
- Desrayaud G., Bennacer R., Caltagirone J.P., Chenier E., Joulin A., Laaroussi N. and K.Mojtabi, Etude numérique comparative des écoulements thermoconvectifs dans un canal vertical chauffé asymétriquement. In VIIIème Colloque Interuniv. Franco-Québécois, Mai 2007, 6 pages.
- Stephan L., Wurtz E., Bastide A., Brangeon B., Jay A., Goffaux C. and Pons C., Benchmark de ventilation naturelle traversante (ADNBATT). Actes Int. Building Performance Simulation Association (IBPSA-France) Conf., 9-10 Novembre 2010, Moret-sur-Loing, France, Ed. J. J. Roux & G. Krauss, Article 'PONS r98.doc', 2010.
- Webb B.W and Hill D.P., High Rayleigh number laminar natural convection in an asymmetrically heated vertical channel. Journal Heat Transfer, (111), 1989, 649–656.
- OpenFOAM 1.7, <http://www.openfoam.com>, 2010.

Nomenclature					
$C_{cell,Ra}$	convective cell center	[-]	U_{CN}	reference velocity	[-]
D_v	mass flow rate	[m ² .h ⁻¹]	x, y	dimensionless spatial coordinate	[-]
G	dimensionless mass flow rate	[-]	Pr	Prandtl number	[-]
g	gravitational acceleration	[m.s ⁻²]	Greek symbols		
H	cavity height	[m]			
H_1, H_2	height inlet and outlet	[m]	β	thermal expansion	[K ⁻¹]
H_3, H_4	height wall East and West	[m]	κ	thermal diffusivity	[m ² .s ⁻¹]
P_m	dimensionless dynamic pressure	[-]	ν	kinematic viscosity	[m ² .s ⁻¹]
Ra	Rayleigh number	[-]	ρ	fluid density	[kg.m ⁻³]
t	dimensionless time	[-]	θ	dimensionless temperature	[-]
T	temperature	[K]	θ_m	dimensionless averaged temperature	[-]
ΔT	temperature difference	[K]			
u, v	dimensionless velocity components	[-]			